Paper 167

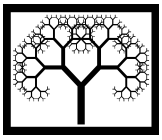

Proceedings of the Eleventh International Conference
on Computational Structures Technology,
B.H.V. Topping, (Editor),
Civil-Comp Press, Stirlingshire, Scotland

Effects of Approximations on the Lateral-Torsional Buckling and Postbuckling Analysis

Y.-L. Pi and M.A. Bradford
Centre for infrastructural Engineering and Safety
School of Civil and Environmental Engineering
The University of New South Wales, Sydney, Australia

Abstract

Lateral-torsional buckling and postbuckling of beams can be analysed using finite element methods. In formulating a finite beam element, a rotation matrix is used to derive nonlinear strain-displacement relationships. Because of couplings between displacements and twist rotations, components of the rotation matrix are lengthy and complicated. To facilitate the formulation, approximations are usually made to simplify the rotation matrix. A simplified small rotation matrix is often used in the lateral-torsional buckling analysis and a simplified second order rotation matrix is used for the lateral-torsional postbuckling analysis. However, the small rotation and second order rotation matrices do not describe rotations accurately and introduce some approximations to the coupling between displacements and rotations. This paper investigates the effects of the approximations on the lateral-torsional buckling and postbuckling analysis of beams. It is shown that a analytical model based on the small rotation matrix predicts incorrect buckling loads. A finite element model based on the second order rotation matrix may lead to poor predictions of the postbuckling behaviour.

Keywords: approximations, lateral-torsional buckling, postbuckling, rotation, second order.

1 Introduction

In development of a finite beam element for the lateral-torsional buckling analysis of structures (Fig. 1), a rotation matrix is usually used to derive the nonlinear strain-displacement relationship. Because of couplings between displacements, twist rotations and their derivatives, the components of the rotation matrix are both lengthy and complicated. To facilitate the formulation, approximations have been used to simplify

the rotation matrix [1]-[7]. A simplified small rotation matrix given by [1, 2]

$$[R] = \begin{bmatrix} 1 & -\phi & u_1' \\ \phi & 1 & u_2' \\ -u_1' & -v_2' & 1 \end{bmatrix} \tag{1}$$

is often used to derive the displacements of an arbitrary point P of the beam as

$$\begin{Bmatrix} u_{P1} \\ u_{P2} \\ u_{P3} \end{Bmatrix} = \begin{Bmatrix} u_1 \\ u_2 \\ u_3 \end{Bmatrix} + [R] \begin{Bmatrix} x \\ y \\ -\omega\phi' \end{Bmatrix} - \begin{Bmatrix} x \\ y \\ 0 \end{Bmatrix}, \tag{2}$$

where u_1, u_2, and u_3 are the lateral, transverse, and axial displacements of the shear centre of a cross-section, ϕ is the twist rotation of the cross-section, u_{P1}, u_{P2}, and u_{P3} are the lateral, transverse, and axial displacements of the point P, x and y are the coordinates of the point P in the principal axis of the cross-section, ω is the normalized section warping displacement, and $(\ )' = \mathrm{d}(\ )/\mathrm{d}z$. The displacements u_{P1}, u_{P2}, and u_{P3} are then used to derive the strains at the point P, which are then used to formulate the total potential energy of a beam and load system for its lateral-torsional buckling and postbuckling analyses.

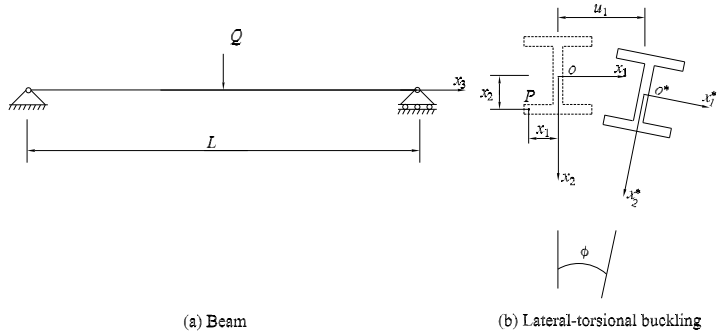

(a) Beam (b) Lateral-torsional buckling

Figure 1: Lateral-torsional buckling.

A second order rotation matrix is conventionally used in the formulation for the buckling and postbuckling analysis of beams and beam-columns [3]-[7], which is given by

$$[R] = \begin{bmatrix} 1 - \frac{1}{2}{u_1'}^2 - \frac{1}{2}\phi^2 & -\phi - \frac{1}{2}u_1'u_2' & u_1' \\ \phi - \frac{1}{2}u_1'u_2' & 1 - \frac{1}{2}{u_2'}^2 - \frac{1}{2}\phi^2 & u_2' \\ -u_1' - u_2'\phi & -u_2' + u_1'\phi & 1 \end{bmatrix}. \tag{3}$$

Because of approximations, these rotation matrices do not satisfy the orthogonality and unimodular conditions. As a result, the approximations may lead to a loss of some significant terms in the nonlinear strain-displacement relationship. Without

these terms, the rigid-space body motion cannot be separated from the real deformations. The superimposed rigid body motions may lead to the development of self-straining, which may in turn affect significantly the prediction of the lateral-torsional buckling loads and the postbuckling behaviour of beams and beam-columns [4, 7]. The aims of this paper are to investigate the effects of approximations on the elastic lateral-torsional buckling and postbuckling analyses of beams and beam-columns and to derive an accurate formulation for the elastic lateral-torsional buckling and post-buckling analyses. Vlasove's theory of torsion [11] and the Euler-Bernoulli theory of bending are used in this paper, i.e. the cross-section of the member maintains its shape during deformation. Another assumption used is that the strains are small.

2 Deformation and Strains

In the formulation of a finite element program for the lateral-torsional buckling and postbuckling analysis of beams and beam-columns, an accurate rotation matrix is required. To derive the rotation matrix, two axis systems are used to describe the motion of a thin-walled member. The first axis system $OX_1X_2X_3$ is fixed in space as shown in Fig. 2. The origin O of the system is located on the centroid of an end of the member. The axis OX_3 coincides with the undeformed centroidal axis of the member. The axes OX_1 and OX_2 coincide with the principal axes ox, oy of the undeformed cross-section. The basis vectors of the axis system $OX_1X_2X_3$ are $\vec{P}_1$, $\vec{P}_2$, $\vec{P}_3$. The second axis system is a body attached axis system. Before deformation, the origin o of the system is at the centroid of a cross-section through $(0, 0, x_3)$ where $0, 0, x_3$ are the coordinates of the origin o in the axis system $OX_1X_2X_3$. The axis ox_3 of the system coincides with the axis OX_3 and the axes ox_1 and ox_2 coincide with the principal axes ox and oy of the cross-section. The basis vectors of the system are $\vec{p}_1, \vec{p}_2, \vec{p}_3$. After deformation, the centroid of the cross-section displace u_1, u_2, u_3 in the direction OX_1, OX_2, OX_3 from the point o to the point o^* and at the same time the cross-section rotates angle ϕ, so that the body-attached axis system moves to $o^*x_1^*x_2^*x_3^*$. The axis $o^*x_3^*$ is in the tangential direction of the deformed centroidal line o^*s^*. The axes $o^*x_1^*$ and $o^*x_2^*$ coincide with the principal axes ox, oy of the cross-section at the deformed position. The basis vectors of the axes system $o^*x_1^*x_2^*x_3^*$ are $\vec{q}_1$, $\vec{q}_2$, $\vec{q}_3$.

The rotation from the vectors $\vec{p}_1, \vec{p}_2, \vec{p}_3$ to the vectors $\vec{q}_1, \vec{q}_2, \vec{q}_3$ can be described by an orthogonal rotation matrix $[R]$

$$\vec{p}_j = [R]\vec{q}_i \qquad (i, j = 1, 2, 3). \tag{4}$$

An accurate rotation matrix was derived by Pi and Trahiar [8] and Pi et al. [9] can be used. The components of of the rotation matrix $[R]$ are given by [8, 9]

$$[R] = \begin{bmatrix} R_{11} & R_{12} & R_{13} \\ R_{21} & R_{22} & R_{23} \\ R_{31} & R_{32} & R_{33} \end{bmatrix}, \tag{5}$$

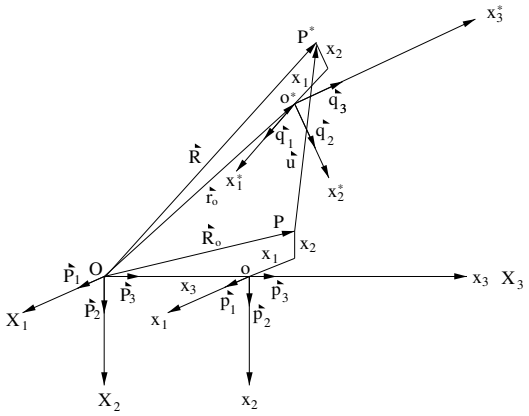

Figure 2: Rotation during deformation.

with

$$R_{11} = [1 - \lambda {u'_1}^2 (1+\epsilon)^{-2}]C - u'_1 u'_2 \lambda (1+\epsilon)^{-2} S, \tag{6}$$

$$R_{12} = -[1 - \lambda {u'_1}^2 (1+\epsilon)^{-2}]S - u'_1 u'_2 \lambda (1+\epsilon)^{-2} C, \tag{7}$$

$$R_{13} = u'_1 (1+\epsilon)^{-1}, \tag{8}$$

$$R_{21} = [1 - \lambda {u'_2}^2 (1+\epsilon)^{-2}]S - u'_1 u'_2 \lambda (1+\epsilon)^{-2} C, \tag{9}$$

$$R_{22} = [1 - \lambda {u'_2}^2 (1+\epsilon)^{-2}]C + u'_1 u'_2 \lambda (1+\epsilon)^{-2} S, \tag{10}$$

$$R_{23} = u'_2 (1+\epsilon)^{-1}, \tag{11}$$

$$R_{31} = -u'_1 (1+\epsilon)^{-1} C - u'_2 (1+\epsilon)^{-1} S, \tag{12}$$

$$R_{32} = u'_1 (1+\epsilon)^{-1} S - u'_2 (1+\epsilon)^{-1} C, \tag{13}$$

$$R_{33} = (1+u'_3)(1+\epsilon)^{-1}, \tag{14}$$

where $C = \cos\phi$, $S = \sin\phi$, ϕ is the twist rotation of the cross-section, $(1+\epsilon)^2 = (u'_1)^2 + (u'_2)^2 + (1+u'_3)^2$, and $\lambda = (1-\cos\alpha)/\sin^2\alpha$ with $\cos\alpha = (1+u'_3)/(1+\epsilon)$.

The rotation matrix in Eq. (5) satisfies the orthogonal conditions $[R][R]^T = [I]$ and $det[R] = 1$ and so it can accurately describe the rotation. An accurate nonlinear finite element model for the 3-D elastic large deformation analysis of beams and beam-columns can be derived based on this rotation matrix.

The second order rotation matrix given by Eq. (3) can also be obtained by introducing approximations $(1+\epsilon) \approx 1$, $\sin\phi \approx \phi$, and $\cos\phi \approx 1 - \phi^2/2$ in the accurate rotation matrix given by Eq. (5) and ignoring the third and higher order terms, while the small rotation matrix given by Eq. (1) can also be obtained by introducing approximations $(1+\epsilon) \approx 1$, $\sin\phi \approx \phi$, and $\cos\phi \approx 1$ in the accurate rotation matrix given by Eq. (5) and ignoring the second and higher order terms.

With the expressions of the displacements of an arbitrary point P given by Eq. (2), the Lagrangian strain components ϵ_{ik} at the point P can be derived as [10]

$$\epsilon_{ii} = \frac{\partial u_{P_i}}{\partial x_i} + \frac{1}{2}\sum_{j=1}^{3}(\frac{\partial u_{P_j}}{\partial x_i})^2 \qquad (i = 1, 2, 3) \tag{15}$$

for normal strains, and

$$\epsilon_{ik} = \frac{\partial u_{P_k}}{\partial x_i} + \frac{\partial u_{P_i}}{\partial x_k} + \sum_{j=1}^{3}\frac{\partial u_{P_j}}{\partial x_i}\frac{\partial u_{P_j}}{\partial x_k} \qquad (i = 1, 2, 3;\ \ k = 2, 3, 1) \tag{16}$$

for shear strains.

Substituting the small rotation matrix given by Eq. (1) into Eqs. (2), (15) and (16) leads to the normal strains as [1, 2]

$$\epsilon_{11} = \epsilon_{22} = 0, \tag{17}$$

and

$$\epsilon_{33} = u_3' + \frac{1}{2}({u_1'}^2 + {u_2'}^2 + {u_3'}^2) - x_1(u_1'' - u_2'\phi') - x_2(u_2'' + u_1'\phi') - \omega\phi'' + \frac{1}{2}(x_1^2 + x_2^2){\phi'}^2; \tag{18}$$

and the shear strains as

$$\epsilon_{12} = 0, \quad \epsilon_{23} = (x_1 - \frac{\partial\omega}{\partial x_2})\phi', \ \text{ and } \ \epsilon_{13} = -(x_2 + \frac{\partial\omega}{\partial x_1})\phi'. \tag{19}$$

Substituting the second rotation matrix given by Eq. (3) into Eqs. (2), (15) and (16) leads to the normal strains as [5]-[6]

$$\epsilon_{11} = \epsilon_{22} = 0, \tag{20}$$

and

$$\epsilon_{33} = u_3' + \frac{1}{2}({u_1'}^2 + {u_2'}^2 + {u_3'}^2) - x_1(u_1'' + u_2''\phi) - x_2(u_2'' - u_1''\phi) - \omega\phi'' + \frac{1}{2}(x_1^2 + x_2^2){\phi'}^2; \tag{21}$$

and the shear strains as

$$\epsilon_{12} = 0, \quad \epsilon_{23} = (x_1 - \frac{\partial\omega}{\partial x_2})\phi', \ \text{ and } \ \epsilon_{13} = -(x_2 + \frac{\partial\omega}{\partial x_1})\phi'. \tag{22}$$

Substituting the accurate rotation matrix given by Eq. (5) into Eqs. (2), (15) and (16), and ignoring the higher order terms lead to the normal strains as [8]

$$\epsilon_{11} = \epsilon_{22} = 0, \tag{23}$$

$$\epsilon_{33} = \{u_3' + \frac{1}{2}({u_1'}^2 + {u_2'}^2 + {u_3'}^2)\} - x_1\{[u_1''\bar{u}_3 - u_1'u_3'']C + [u_2''\bar{u}_3 - u_2'u_3'']S\}$$
$$+ x_2\{[u_1''\bar{u}_3 - u'u_3'']S - [u_2''\bar{u}_3 - u_2'u_3'']C\} - \omega\{\phi' - \frac{1}{2}(u_1''u_2' - u_1'u_2'')\}'$$
$$+ \frac{1}{2}({x_1}^2 + {x_2}^2)\phi'^2; \tag{24}$$

and the shear strains as

$$\epsilon_{12} = 0, \tag{25}$$

$$\epsilon_{23} = (x_1 - \frac{\partial\omega}{\partial x_2})[\phi' + \frac{1}{2}(u_1''u_2' + u_1'u_2'')], \tag{26}$$

and

$$\epsilon_{13} = -(x_2 + \frac{\partial\omega}{\partial x_1})[\phi' + \frac{1}{2}(u_1''u_2' + u_1'u_2'')] \tag{27}$$

with $\bar{u}_3 = 1 + u_3'$.

The Vlasov's hypothesis [11] that the shear deformations in the mid-surface of the thin-walled plate are extremely small and can be neglected is used for open thin-walled members. According to this hypothesis, the warping function $\omega(x_1, x_2)$ have different expressions for the different thin-walled plates of the cross-section. For example, for I-section,

$$\omega(x_1, x_2) = \begin{cases} x_1(x_2 + h) & \text{for top flange} \\ -x_1x_2 & \text{for web} \\ x_1(x_2 - h) & \text{for bottom flange} \end{cases} \tag{28}$$

where h is the distance between the centroids of top and bottom flanges.

3 Lateral-Torsional Buckling Analysis

The potential energy of the system in the infinitesimal lateral-torsional buckling configuration can be expressed as

$$\Pi = \int_V \left\{\frac{1}{2}[E\epsilon_{33}^2 + G(\epsilon_{13}^2 + \epsilon_{23}^2)] + \sigma_{33}\epsilon_{33}\right\} \mathrm{d}V, \tag{29}$$

where the first term is the strain energy due to lateral-torsional buckling deformations and the second term is the energy due to the constant prebuckling stress $\sigma_{33} = E\epsilon_{33}$ associated with the strain ϵ_{33} produced by the lateral-torsional buckling deformations.

For a beam with a uniform doubly symmetric I-section, by substituting Eqs. (18)-(19) into Eq. (29), and ignoring the higher order terms, the potential energy based on the small rotation model given by Eq. (29) can be rewritten as a functional by

$$\Pi = \frac{1}{2}\int_0^L (EI_2u_1''^2 + GJ\phi'^2 + EI_w\phi''^2 - 2Mu_1'\phi')\mathrm{d}z \tag{30}$$

where $I_2 = \int\int y^2 \mathrm{d}A$, $J = \int\int[(x_1 - \partial\omega/\partial x_2)^2 + (x_2 + \partial\omega/\partial x_1)^2]\mathrm{d}A$, $I_w = \int\int \omega^2 \mathrm{d}A$, and $M = \int\int \sigma_{33} x_2 \mathrm{d}A$.

Substituting Eqs. (21) and (22) into Eq. (29) leads to the total potential energy based on the second rotation matrix as

$$\Pi = \frac{1}{2}\int_0^L (EI_2 u_1''^2 + GJ\phi'^2 + EI_w\phi''^2 - 2Mu_1''\phi)\mathrm{d}z. \tag{31}$$

The term $\int_0^L 2Mu_1'\phi'\mathrm{d}z$ of the small rotation model in Eq. (30) for the work done by the stress resultant during the buckling is quite different from the corresponding term $\int_0^L 2Mu_1''\phi\mathrm{d}z$ of the second order model in Eq. (31). This difference will affect the predictions of the lateral-torsional buckling load of a beam. To illustrate this, the lateral-torsional buckling of a simply supported beam of doubly symmetric I-section under a moment gradient is investigated (Fig. 3). The moment in the beam can be expressed as

$$M(z) = M\left[1 - (1+\beta)\frac{z}{L}\right]. \tag{32}$$

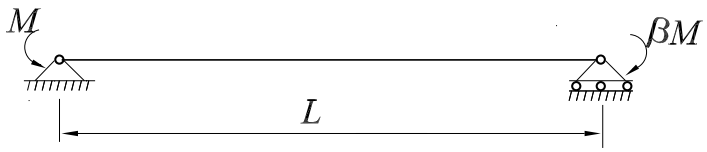

Figure 3: Simply supported beam under moment gradient.

The buckling shapes of the beam may be approximated as

$$\phi = \theta \sin\frac{\pi z}{L} \quad \text{and} \quad u_1 = \delta_1 \sin\frac{\pi z}{L} + \delta_2 \sin\frac{2\pi z}{L}. \tag{33}$$

By substituting Eq. (33) into Eq. (30), the potential energy can be expressed as a function of δ_1, δ_2 and θ by

$$\Pi = \frac{\pi^2}{L^3}\left\{\frac{N_2}{4}\delta_1^2 + 4N_2\delta_2^2 + \frac{r_0^2 N_3}{4}\theta^2 - \frac{20M}{9\pi^2}(\beta-1)\delta_2\theta + \frac{M}{4}(\beta-1)\delta_1\theta\right\}, \tag{34}$$

in which N_2 and N_3 are the flexural buckling load and the torsional buckling load of the pin-ended column with the same length under uniform axial compression, respectively; and they are given by

$$N_2 = \frac{EI_2\pi^2}{L^2} \quad \text{and} \quad N_3 = \frac{1}{r_0^2}\left(GJ + \frac{EI_w\pi^2}{L^2}\right) = 0. \tag{35}$$

Minimization of the function Π given by Eq. (34) is equivalent to minimization of the potential energy given by Eq. (30). The values of $\delta_1, \delta_2, \theta$ minimizing the function

Π should therefore satisfy the algebraic equations

$$\frac{\partial \Pi}{\partial \delta_1} = 0, \quad \frac{\partial \Pi}{\partial \delta_2} = 0, \text{ and } \frac{\partial \Pi}{\partial \theta} = 0 \tag{36}$$

which leads to the matrix eigenvalue problem as

$$\frac{1}{2}\frac{\pi^2}{L^3}\begin{bmatrix} N_2 & 0 & M_a \\ 0 & 16N_2 & M_b \\ M_a & M_b & r_0^2 N_3 \end{bmatrix}\begin{Bmatrix} \delta_1 \\ \delta_2 \\ \theta \end{Bmatrix} = \begin{Bmatrix} 0 \\ 0 \\ 0 \end{Bmatrix} \tag{37}$$

where $M_a = -M[1-(1+\beta)/2]$ and $M_b = -0.36025M(1+\beta)$.

Non-trivial solution for $\{\delta_1, \delta_2, \theta\}^T$ requires that the determinant of the coefficient matrix of Eq. (37) vanishes, which leads to the solution for the lateral-torsional buckling of the beam as

$$\frac{M_{cr}}{M_{23}}\sqrt{\frac{1}{[1-(1+\beta)/2]^2 + [0.09005(1+\beta)]^2}}, \tag{38}$$

where $M_{23} = \sqrt{r_0^2 N_2 n_3}$ is the lateral-torsional buckling moment of a simply supported beam under uniform bending.

When the second order rotation matrix is used, the matrix eigenvalue problem becomes

$$\frac{1}{2}\frac{\pi^2}{L^3}\begin{bmatrix} N_2 & 0 & M_a \\ 0 & 16N_2 & M_c \\ M_a & M_c & r_0^2 N_3 \end{bmatrix}\begin{Bmatrix} \delta_1 \\ \delta_2 \\ \theta \end{Bmatrix} = \begin{Bmatrix} 0 \\ 0 \\ 0 \end{Bmatrix} \tag{39}$$

where $M_c = -0.7205M(1+\beta)$.

Accordingly, the solution for the lateral-torsional buckling of the beam becomes

$$\frac{M_{cr}}{M_{23}}\sqrt{\frac{1}{[1-(1+\beta)/2]^2 + [0.1801(1+\beta)]^2}}. \tag{40}$$

The solution based on the small rotation matrix given by Eq. (38) is compared with that based on the second order rotation matrix given by Eq. (40) in Fig. 4. The FE results of of the finite beam element developed in this paper and ABAQUS [12] are also shown in Fig. 4. In the FE analysis, the Australian steel 250UB37 I-section [13] was chosen as the cross-section of these arches and its dimensions are: the overall depth $D = 256$ mm, the flange width $B = 146$ mm, the flange thickness $t_f = 10.9$ mm, the web thickness $t_w = 6.4$ mm, and the radius of gyration of the cross-section about its major principal axis (x axis) $r_x = 108$ mm. The Young's and shear moduli were assume as $E = 200,000$ MPa and $G = 80,000$ MPa. The FE results of the present finite beam element are indentical to those of ABAQUS [12]. It can be seen that the solution given by Eq. (40) agrees with the FE results extremely well while the solution given by Eq. (38) over-estimates the buckling moments when the moment gradient coefficient $\beta \geq -0.4$.

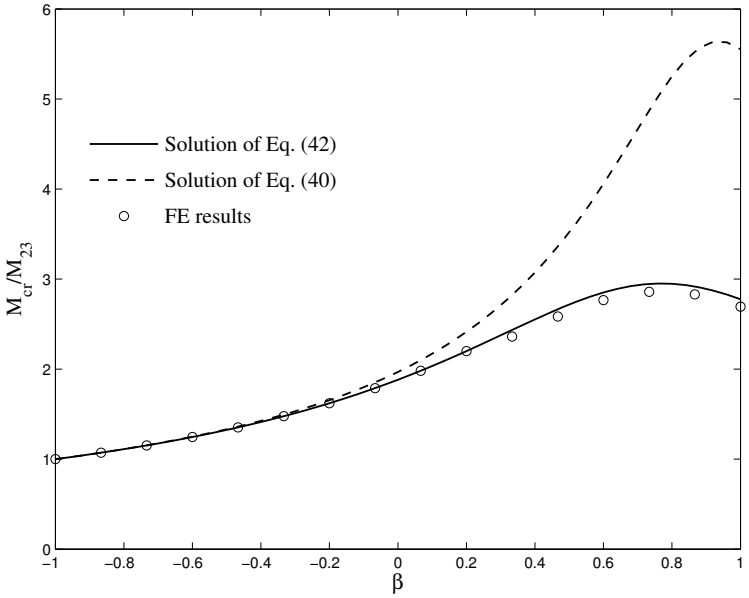

Figure 4: Lateral-torsional buckling of simply supported beam.

4 Lateral-Torsional Postbuckling Analysis

4.1 Nonlinear equilibrium

To predict the lateral-torsional postbuckling behaviour of beams and beam-columns, a finite element for the nonlinear elastic large deformation needs to be developed. For this, the nonlinear equilibrium equations of a beam or beam-column can be derived from the principle of virtual work that requires that

$$dU = \int\int\int \{d\epsilon\}^T \{\sigma\} dV - \{dr\}^T \{Q\} = 0 \tag{41}$$

for all sets of virtual displacements $\{dr\}$ and corresponding virtual strains $\{d\epsilon\}$, where $\{r\}$ is the nodal displacement vector given by

$$\{r\} = \{u_{11}, u'_{11}, u_{12}, u'_{12}, u_{13}, \phi_1, \phi'_1, u_{21}, u'_{21}, u_{22}, u'_{22}, u_{23}, \phi_2, \phi'_2\}^T, \tag{42}$$

and $\{Q\}$ are the corresponding nodal forces which are equivalent to the applied actions.

The variations of finite strains $\{d\epsilon\}$ can be obtained from Eqs. (24), (26) and (27) as

$$\{d\epsilon\} = \{d\epsilon_{33}, d\epsilon_{23}, d\epsilon_{13}\}^T = [S][B]\{d\theta\}, \tag{43}$$

where

$$\{d\theta\} = \{du'_1, du''_1, du'''_1, du'_2, du''_2, du'''_2, du'_3, du''_3, d\phi, d\phi', d\phi''\}^T, \tag{44}$$

$$[S] = \begin{bmatrix} 1 & x_1 & x_2 & \omega & (x_1^2 + x_2^2) & 0 \\ 0 & 0 & 0 & 0 & 0 & (x_1 - \partial\omega/\partial x_2) \\ 0 & 0 & 0 & 0 & 0 & -(x_2 + \partial\omega/\partial x_1) \end{bmatrix}, \tag{45}$$

and the components of matrix $[B]$ are dependent on the rotation matrix used.

Substituting Eq. (43) into (41) and introducing

$$\{\theta\} = [N]\{r\} \tag{46}$$

leads to the nonlinear equilibrium equations

$$\{Q\}_{int} - \{Q\} = \{0\} \quad \text{with} \quad \{Q\}_{int} \int_0^L [N]^T [B]^T \{R\} dx_3, \tag{47}$$

where $[N]$ is the shape function matrix whose elements are the functions of z, and $\{R\}$ is the stress resultant vector defined by

$$\{R\} = \int\int [S]^T \{\sigma\} dA. \tag{48}$$

Taking variations of Eq. (47) leads to the nonlinear incremental equilibrium equations

$$[k_T]\{\Delta r\} = \{\Delta Q\} \tag{49}$$

where the tangent stiffness matrix $[k]_T$ is given by

$$[k]_T = [k] + [k]_G, \tag{50}$$

in which $[k]$ is the displacement stiffness matrix given by

$$[k] = \int_0^L [N]^T [B]^T [D][B][N] dx_3 \quad \text{with} \quad [D] = \int\int [S]^T [E]^{ep} [S] dA, \tag{51}$$

and $[k]_G$ is the geometric stiffness matrix given by

$$[k]_G = \int_0^L [N]^T [M]_\sigma [N] dx_3, \tag{52}$$

with the following identity

$$[dB]^T \{R\} = [M]_\sigma \{d\theta\} = [M]_\sigma [N]\{dr\} \tag{53}$$

being used.

Equations (49) can be used for both the conventional second order finite beam element and the present accurate finite element models. However, the matrix $[B]$ in the displacement stiffness matrix $[k]$ and the matrix $[M]_\sigma$ in the geometric stiffness matrix $[k]_G$ are different and these differences may have significant effects of the elastic lateral-torsional postbuckling analysis of beams and beam-columns. The details of thses differences are given in the next section.

4.2 Effects of approximations on the stiffness matrix

To illustrate further how some significant terms are lost in the conventional second order rotation model, a term $-x_2[u_2''(1+u_3') - u_2'u_3''] \cos\phi$ of the longitudinal normal strains ϵ_{33} of the accurate rotation model given in Eq. (24) and the corresponding term $-x_2u_2''$ of the second order rotation model given in Eq. (21) are herein used.

The first variation of these terms contributes to the displacement stiffness matrix $[k]$ can be written as

$$[k]_{x2} = \int_0^L [N]_\sigma^T [B]_{x_2}^T [D][B]_{x_2}[N]_\sigma dx_3. \tag{54}$$

The first variation of the term $-x_2[u_2''(1+u_3') - u_2'u_3''] \cos\phi$ of the accurate rotation model is

$$\delta\left\{-x_2[u_2''(1+u_3') - u_2'u_3''] \cos\phi\right\} =$$
$$-x_2[u_2''\delta u_3' + (1+u_3')\delta u_2'' - u_2'\delta u_3'' - u_3''\delta u_2'] \cos\phi + x_2[u_2''(1+u_3') - u_2'u_3''] \sin\phi\delta\phi, \tag{55}$$

and its contribution to the matrix $[B]$ is

$$[B]_{x_2} = \begin{bmatrix} 0 & 0 & 0 & 0 & 0 & 0 & 0 & 0 & 0 & 0 & 0 \\ 0 & 0 & 0 & 0 & 0 & 0 & 0 & 0 & 0 & 0 & 0 \\ 0 & 0 & 0 & u_3''C & -(1+u_3')C & 0 & -u_2''C & u_2'C & u_2''S & 0 & 0 \\ 0 & 0 & 0 & 0 & 0 & 0 & 0 & 0 & 0 & 0 & 0 \\ 0 & 0 & 0 & 0 & 0 & 0 & 0 & 0 & 0 & 0 & 0 \\ 0 & 0 & 0 & 0 & 0 & 0 & 0 & 0 & 0 & 0 & 0 \end{bmatrix} \tag{56}$$

where $C = \cos\phi$, $S = \sin\phi$, and third and higher order terms are omitted.

The first variation of the term $-x_2u_2''$ of the second order rotation model is

$$\delta(-x_2u_2'') = -x_2\delta u_2'', \tag{57}$$

and its contribution to the matrix $[B]$ is

$$[B]_{x_2} = \begin{bmatrix} 0 & 0 & 0 & 0 & 0 & 0 & 0 & 0 & 0 & 0 & 0 \\ 0 & 0 & 0 & 0 & -1 & 0 & 0 & 0 & 0 & 0 & 0 \\ 0 & 0 & 0 & 0 & 0 & 0 & 0 & 0 & 0 & 0 & 0 \\ 0 & 0 & 0 & 0 & 0 & 0 & 0 & 0 & 0 & 0 & 0 \\ 0 & 0 & 0 & 0 & 0 & 0 & 0 & 0 & 0 & 0 & 0 \\ 0 & 0 & 0 & 0 & 0 & 0 & 0 & 0 & 0 & 0 & 0 \end{bmatrix}. \tag{58}$$

Comparison Eq. (56) with Eq. (58) indicates that all the nonlinear terms of the matrix $[B]_{x2}$ given by Eq. (56) are lost in the second order rotation model.

The second variation of the terms $-x_2[u_2''(1+u_3') - u_2'u_3'']\cos\phi$ and $-x_2u_2''$ contributes to the geometric stiffness matrix $[k]_G$ as

$$[k]_{G_{x2}} = \int_0^L [N]_\sigma^T [M]_{\sigma_{x_2}} [N]_\sigma dx_3. \tag{59}$$

The second variation of the term $-x_2[u_2''(1+u_3') - u_2'u_3'']\cos\phi$ of the accurate rotation model is equal to

$$\delta\{-x_2[u_2''(1+u_3') - u_2'u_3'']\cos\phi\} = 2x_2[u_2''\delta u_3' + (1+u_3')\delta u_2'' - u_2'\delta u_3'' - u_3''\delta u_2']\sin\phi\delta\phi$$
$$-2x_2(\delta u_2''\delta u_3' - \delta u_2'\delta u_3'')\cos\phi + x_2[u_2''(1+u_3') - u_2'u_3'']\cos\phi(\delta\phi)^2, \tag{60}$$

and its contribution to matrix $[M]$ is

$$[M]_{\sigma_{x_2}} = \begin{bmatrix} 0 & 0 & 0 & 0 & 0 & 0 & 0 & 0 & 0 & 0 & 0 \\ & 0 & 0 & 0 & 0 & 0 & 0 & 0 & 0 & 0 & 0 \\ & & 0 & 0 & 0 & 0 & 0 & 0 & 0 & 0 & 0 \\ & & & 0 & 0 & 0 & 0 & R_3\cos\phi & 0 & 0 & 0 \\ & & & & 0 & 0 & -R_3\cos\phi & 0 & R_3\sin\phi & 0 & 0 \\ & & & & & 0 & 0 & 0 & 0 & 0 & 0 \\ & & & & & & 0 & 0 & 0 & 0 & 0 \\ & & & & & & & 0 & 0 & 0 & 0 \\ & & & & & & & & 0 & 0 & 0 \\ & & & & & & Sym. & & & 0 & 0 \\ & & & & & & & & & & 0 \end{bmatrix} \tag{61}$$

where the effects of third and higher order terms are omitted, and

$$R_3 = \int\int x_2\sigma_{33}dA. \tag{62}$$

The second variation of the term $-x_2u_2''$ of the second order rotation model is equal to zero so that it has no contribution to the matrix $[M]$ and

$$[M]_{\sigma_{x2}} = [0], \tag{63}$$

which shows that all the significant terms of the geometric stiffness matrix $[k]_G$ due to Eq. (61) are completely lost in the second order rotation model.

4.3 Incremental-iterative analysis

A Newton-Raphson method is used in conjunction with the incremental equilibrium equation given by Eq. (49) to solve the nonlinear equilibrium equations (Eq. (47)). In the incremental-iterative implementation, each load step consists of the application of

an increment of the external loads and subsequent iterations to correct the errors until the nonlinear equilibrium is restored within a specified admissible tolerance. Before the restoration, the internal and external forces are not in equilibrium and hence the incremental-iterative equilibrium equations can be written from Eq. (49) as

$$[k]_i\{\Delta r\}_i^j = \{\Delta Q\}_i + \{\Delta Q\}_i^{j-1}, \tag{64}$$

where i and j denote the load step and the iteration within the load step, respectively, and $\{\Delta Q\}_i^{j-1}$ is the unbalanced force in the last iteration $(j-1)$ that can be calculated using Eq. (47) as

$$\{\Delta Q\}_i^{j-1} = [Q_{in} - Q]_i^{j-1}. \tag{65}$$

The arc-length method is used as the iterative strategy, with an automatic increment of the arc-length being used as the incremental strategy [8, 9, 14]. The sign of the determinant of the tangent stiffness matrix is used for the sign of the load increment. The maximum norm of the incremental displacements is used for testing the convergence, so that

$$||\epsilon|| = \max_k |\frac{\Delta r_k}{r_{k,ref}}| < \zeta \tag{66}$$

where Δr_k is the change in the displacement component k during the current iteration cycle, $r_{k,ref}$ is the largest displacement component of the corresponding type, and ζ is in the range 10^{-2} to 10^{-5}, depending on the desired accuracy.

4.3.1 Buckling and postbuckling analysis of an elastic continuous beam

The flexural-torsional buckling and postbuckling behaviours of an elastic aluminium I-section two span continuous beam subjected to concentrated loads Q_1 and Q_2 at mid-spans D and E of each span shown in Figs. 5 and 6 were investigated. The loads Q_1 and Q_2 are applied at $x_{2q} = -41.1$ mm and the load ratio is $Q_1/Q_2 = 0.5$. The self-weight of the beam is $q_{x_2} = 77.874$ N/m. To induce flexural-torsional buckling, small initial out-of-plane crookedness ($u_{1_o} = u_{1_{oc}} \sin \pi x_3/L$ with $u_{1oc} = L/1,000,000$) is introduced. The beam is divided into eight equal elements.

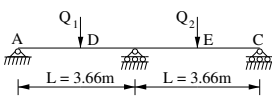

Figure 5: Two span continuous beam.

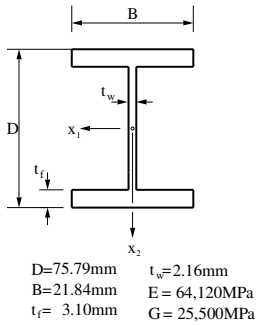

Figure 6: Cross-section.

The results of the present accurate and conventional second order models are compared with the test results of Woolcock and Trahair [15] in Fig. 7 where Q is the value of Q_2, Q_{cr} is the test elastic buckling load of Q_2, and u_{x_1} is the lateral displacements of the points D and E. The buckling loads predicted by both the accurate and the conventional second order models are almost identical and agree well with the test result. However, for the postbuckling behaviour, the results of the conventional second order model are significantly different from those of the present accurate model. The results of the present accurate model are in very good agreements with the test results, but the results of the conventional second order model are over-stiff and their agreements with the test results are poor.

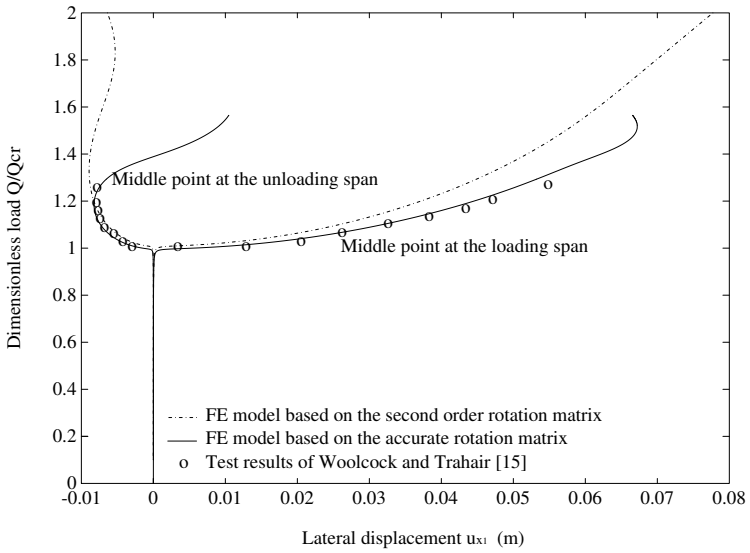

Figure 7: Lateral-torsional buckling of two span continuous beam.

5 Conclusions

The effects of approximations in formulating a finite element model on the nonlinear inelastic large rotation analysis of beams and beam-columns have been investigated in this paper. A total Lagrange nonlinear finite element model for the three-dimensional analysis of beams and beam-columns has been developed. No approximations were made in deriving the nonlinear strains so that some significant contributions to the tangent stiffness matrix by the coupling terms and the higher order curvatures have been retained. As a result, the over-stiff solutions have been eliminated. In a conventional model, however, these significant contributions have been lost because of approximations in the formulation. Comparisons with available experimental and analytical results have shown that the approximations may lead to over-estimations of the buckling loads of beams, and poor postbuckling analysis of beams and beam-columns in some cases.

Acknowledgement

This work has been supported by the Australian Research Council through Discovery Projects (DP1097096 and DP1096454) awarded to the authors and a Laureate Fellowship (FL100100063) awarded to the second author.

References

[1] Timoshenko, S.P., and Gere, J.M. (1961), Theory of elastic stability. 2nd. ed., McGraw-Hill, New York, NY(1961).

[2] Gellin, S. Lee, G.C., and Chern, J.H. (1983), "A finite element model for thin-walled members", Computers and Structures, 19(1), 59-71.

[3] Kitipornchai, S. and Chan, S.L. (1990), "Stability and nonlinear finite element analysis", in Finite element applications to thin walled structures, ed. by J.W. Bull, Elsevier Applied Science, London, England, 89-130.

[4] Pi, Y.-L., Trahair, N.S., and Rajasekaran, S. (1992), "Energy equation for beam lateral buckling", Journal of Structural Engineering, ASCE, 118(7), 1462-1479.

[5] Bild, S., Chen, G., and Trahair, N.S. (1992), "Out-of-plane strength of steel beams", Journal of Structural Engineering, ASCE, 118(8), 1987-2003.

[6] Pi, Y.L., and Trahair, N.S. (1992), "Prebuckling deflections and lateral buckling. I: theory", Journal of Structural Engineering, ASCE, 118(11), 2949-296.

[7] Pi, Y.L., and Trahair, N.S. (1992), "Prebuckling deflections and lateral buckling. II: applications", Journal of Structural Engineering, ASCE, 118(11), 2967-2985.

[8] Pi, Y.L., and Trahair, N.S. (1994), "Nonlinear inelastic analysis of steel beam-columns - theory", Journal of Structural Engineering, ASCE, 120(7), 2041-2061.

[9] Pi, Y.L., Bradford, M.A., and Uy B (2005), "A spatially curved-beam element with warping and Wagner effects", International Journal for Numerical Methods in Engineering, 63, 1342-1369.

[10] Timoshenko, S.P. and Goodier, J.N. (1970, Theory of Elasticity, 3rd edn, McGraw-Hill, New York.

[11] Vlasov, V.Z. (1961), Thin-walled elastic beams. 2nd ed., Israel Program for Scientific Translation, Jerusalem.

[12] ABAQUS (2008), ABAQUS Standard User's Manual version 6.7, Hibbit, Karlsson and Sorensen Inc., Abaqus, Pawtucket, Rhode Island.

[13] BHP, BHP (2000), Hot rolled and structural steel products. 2000 Edition, BHP Co. Pty Ltd, Melbourne.

[14] Crisfield, M.A. (1990), "A consistent co-rotational formulation for non-linear, three-dimensional beam-elements", Comp. Methods Appl. Engrg., 81, 131-150.

[15] Woolcock, S.T., and Trahair, N.S. (1976), "Post-buckling of redundant I-beams", Journal of Engineering Mechanics Division, ASCE, 102(2), 293-312.